SCIENTIFIC BULLETIN OF THE LODZ UNIVERSITY OF TECHNOLOGY
No. 1210 Physics, Vol. 37 2016

GRZEGORZ DERFEL, MARIOLA BUCZKOWSKA

Institute of Physics, Lodz University of Technology, Wólczańska 219
90-924 Łódź, Poland, e-mail: mbuczkow@p.lodz.pl

TWO-DIMENSIONAL DEFORMATIONS IN TWISTED FLEXOELECTRIC NEMATIC CELLS

Electric field induced deformations occurring in twisted nematic cells filled with liquid crystalline material possessing flexoelectric properties were simulated numerically. The aim of computations was to compare the two-dimensional periodic deformations with one-dimensional distortions reported in our earlier paper occurring in the same cells. It was found that the periodically deformed structures have lower free energy counted per unit area of the layer than the one-dimensional deformations.

Keywords: twisted nematic, flexoelectricity, periodic patterns.

1. INTRODUCTION

Twisted nematic cells are fundamental for construction of liquid crystal displays. The deformations of the twisted director field occurring under bias voltage are crucial for operation of electro-optic liquid crystal devices. Their development under the action of external electric field is well known [1,2]. Nevertheless, if the nematic material possesses flexoelectric properties [3,4], the deformations reveal some novel features. They are interesting because flexoelectricity can become essential feature of a nematic mixture if it contains mesogenic substances composed of bent-core molecules which exhibit giant flexoelectric properties [5,6].

In our previous paper [7] we reported the results of numerical simulations which concerned deformations of four particular twisted flexoelectric nematic cells. The problem was considered as one-dimensional. In the present paper, we consider the same cells characterized by the same sets of parameters, however we adopt another approach, i.e. we investigate occurring of two-dimensional deformations. Such two-dimensional deformations take the form of periodic pattern and can be seen under microscope as parallel stripes. They were detected experimentally in planar, homeotropic, twisted and super-twisted nematic layers.

In some cases, the periodic deformations were attributed to flexoelectricity [8-12], nevertheless they can arise in various configurations without contribution of flexoelectricity and were observed in magnetic field as well [13-16]. The deformation in the form of stripes is undesirable effect which destroys uniform appearance over area of an excited pixel of a LCD [17]. The comprehensive review of the periodic patterns of various nature is given by Hinov et al. [18]. Role of flexoelectricity in pattern formation is described in [4]. Structure and properties of periodic pattern were the subject of many theoretical and numerical studies [19-27].

The aim of this paper is to compare the two-dimensional periodic deformations with one-dimensional distortions which occurred in the same cells and were described in our earlier paper [7]. It is shown that the periodically deformed structures have lower free energy than the one-dimensional deformations.

2. ASSUMPTIONS AND METHOD

The twisted nematic structure of thickness d confined between two plane electrodes parallel to the xy plane of Cartesian coordinate system positioned at $z = \pm d/2$ was considered. We assumed that all the physical quantities and variables describing the two dimensional structures depended on two coordinates, y and z, and were constant along the x axis. The director distribution $\mathbf{n}(y,z)$ was determined by means of the polar angle $\theta(y,z)$ measured between $\mathbf{n}$ and the xy plane and by the azimuthal angle $\phi(y,z)$ made between the x axis and the projection of $\mathbf{n}$ on the xy plane. Voltage U was applied between the electrodes. The lower electrode was earthed, i.e. $V(-d/2) = 0$. Boundary conditions were determined by the polar and azimuthal angles θ_{s1}, θ_{s2}, ϕ_{s1} and ϕ_{s2} which determined orientation of the easy axes $\mathbf{e_1}$ and $\mathbf{e_2}$ on the lower and upper electrode, respectively. The anisotropic surface anchoring, expressed by the formula proposed in [7], was assumed. The anchoring energy was determined by polar and azimuthal anchoring strengths, $W_{\theta 1}$, $W_{\phi 1}$, $W_{\theta 2}$, $W_{\phi 2}$ and by means of dimensionless anisotropy parameters $w_i = W_{\theta i} / W_{\phi i}$, $i = 1,2$. The elastic constants, the flexoelectric coefficients of nematic and the surface tilt angles were identical in all the cells: $k_{11} = 6$ pN, $k_{22} = 4$ pN, $k_{33} = 9$ pN, $e_{11} = 0$, $e_{33} = -40$ pC/m, $\theta_{s1} = \theta_{s2} = \theta_s = 0.5°$. Other parameters of the layers are gathered in Table 1. The presence of ions was neglected, i.e. the nematic was treated as perfect insulator. The equilibrium structures of the director field inside the layer were determined by minimization of the free energy counted per unit area of the layer. For this purpose, we used the method which was successfully

Table 1

Parameters of the layers

	Cell A	Cell B	Cell C	Cell D
$\Delta\varepsilon$	4	4	4	8
$W_{\theta 1}$ [J/m^2]	10^{-4}	10^{-4}	10^{-4}	3.3×10^{-4}
$W_{\phi 1}$ [J/m^2]	10^{-5}	5×10^{-5}	10^{-4}	3.3×10^{-5}
$W_{\theta 2}$ [J/m^2]	2×10^{-5}	2×10^{-5}	2×10^{-5}	5×10^{-5}
$W_{\phi 2}$ [J/m^2]	2×10^{-6}	10^{-5}	2×10^{-5}	5×10^{-6}
w	10	2	1	10
d [μm]	3.50	3.30	3.245	2.32
$\phi_{s2} - \phi_{s1}$	90°	90°	90°	86.6°

applied in earlier works [23,24]. A single stripe of width λ was considered during the computations. It was parallel to the *x* axis which means that the wave vector **q** of the periodic structure was directed along the *y* axis. The periodic boundary conditions along the *y* axis were imposed. The free energy of a single stripe was expressed as a function of the set of variables which contained the discrete angles θ_{ij} and ϕ_{ij} defined in sites of the regular lattice, the spatial period of deformations λ and the angle $\psi = (\phi_{s2} + \phi_{s1})/2$ between the stripes and the average direction of the easy axes $\mathbf{e} = (\mathbf{e_1} + \mathbf{e_2})/|\mathbf{e_1} + \mathbf{e_2}|$. Energy of the stripe was divided by λ in order to obtain the total free energy per unit area of the layer:

$$
\begin{aligned}
F = \frac{1}{2\lambda}\int_0^{\lambda}\Bigg\{ \int_{-d/2}^{d/2}\Big\{ & k_{11}(\nabla\mathbf{n})^2 + k_{22}\left[\mathbf{n}\cdot(\nabla\times\mathbf{n})\right]^2 + k_{33}\left[\mathbf{n}\times(\nabla\times\mathbf{n})\right]^2 \\
& - 2\left[e_{11}\mathbf{n}\cdot\nabla\mathbf{n} - e_{33}\mathbf{n}\times(\nabla\times\mathbf{n})\right]\cdot\mathbf{E} - \frac{1}{2}\varepsilon_0\varepsilon_\perp E^2 - \varepsilon_0\Delta\varepsilon(\mathbf{n}\cdot\mathbf{E})^2 \Big\}\mathrm{d}z \Bigg\}\mathrm{d}y \\
& + \frac{1}{2\lambda}\int_0^{\lambda}\Big\{\left[W_{\phi 1}\cos^2(\theta_1 - \theta_{s1}) + W_{\theta 1}\sin^2(\theta_1 - \theta_{s1})\right]\left[1 - (\mathbf{n_1}\cdot\mathbf{e_1})^2\right]\Big\}\mathrm{d}y \\
& + \frac{1}{2\lambda}\int_0^{\lambda}\Big\{\left[W_{\phi 2}\cos^2(\theta_2 - \theta_{s2}) + W_{\theta 2}\sin^2(\theta_2 - \theta_{s2})\right]\left[1 - (\mathbf{n_2}\cdot\mathbf{e_2})^2\right]\Big\}\mathrm{d}y
\end{aligned}
\tag{1}
$$

where $\mathbf{n_1}$, $\mathbf{n_2}$ denote the directors adjacent to the lower and upper plate, respectively whereas θ_1 and θ_2 are their polar orientation angles.

The final set of the *v*ariables, which approximated the real equilibrium director distribution, was calculated in the course of an iteration process during which these variables were varied successively by small intervals. The free energy per unit area of the layer was calculated after each change. New values of the variables were accepted if they led to the lower free energy. This procedure was repeated until no further reduction in the total free energy could be achieved. Then the interval was decreased and the process was repeated. As a result,

a state with minimum energy, characterized by the angles θ_{ij} and ϕ_{ij}, spatial period λ and orientation of the stripes ψ, was obtained.

The electric potential distribution $V(y,z)$ in the layer was calculated by resolving the Poisson equation written here in compact form:

$$\frac{\partial}{\partial y}\frac{\partial g_{el}}{\partial V_y}+\frac{\partial}{\partial z}\frac{\partial g_{el}}{\partial V_z}=0 \tag{2}$$

where g_{el} is the electric part of the bulk free energy density, $V_y=\partial V/\partial y$, $V_z=\partial V/\partial z$, $V(-d/2)=0$ and $V(d/2)=U$ where $U>0$.

3. RESULTS

In all the four layers a small one-dimensional deformations appeared at low voltages starting from $U=0$, due to the non zero tilt angles $\theta_{s1}=\theta_{s2}=0.5°$. Two different types of two-dimensional deformations were found. The first type, which we denote as Type 1, arose on the background of the one-dimensional distortions at some threshold voltage U_1. The calculations showed that above this threshold the energy of the periodic deformations was lower than that of the one-dimensional deformations which would arise at the same voltage. The dependence of the angles θ and ϕ on y coordinate can be approximated by functions proportional to $\sin(2\pi y/\lambda)$ and $\cos(2\pi y/\lambda)$ respectively. Maximum amplitude of this variation reached c. 40°. The stripes orientation angle ψ depended on voltage and varied between c. 10° and 30°. The spatial period decreased with increasing voltage. This form of distortion developed up to some higher threshold, U_2. The second type of the periodic deformations, denoted as Type 2, appeared rapidly at this threshold. The energy per unit area decreased although the distortion became much stronger. Variation of the angles θ and ϕ along the y coordinate differed significantly from sinusoidal. Maximum amplitude of variation tended to c. 90°. The stripes of Type 2 were oriented at ψ = 45° with respect to the vector **e**, i.e. they were perpendicular to the y axis and simultaneously parallel to the easy axis $\mathbf{e_1}$, where the anchoring was stronger. The spatial period decreased farther with voltage. When the voltage was lowered, the Type 2 pattern was maintained below U_2, which led to hysteresis. The stripes became wider with decreasing voltage and they kept constant orientation ψ = 45°.

The structure of stripes is determined by the functions $\theta(y,z)$, $\phi(y,z)$. However for simplicity, we present the deformations by y-dependence of the angles $\theta(z=d/2)$ and $\phi(z=d/2)$ which determine polar and azimuthal orientations of director adjacent to the upper electrode where the anchoring is

weaker than that on the lower plate. In Fig. 1a, the profiles characterizing the periodic pattern of both types arising in the cell A for low and high voltage are illustrated by means of those angles plotted as a function of reduced coordinate y/λ. In Fig. 1b, the structure of the stripe of Type 2 is presented by means of cylinders symbolizing the director.

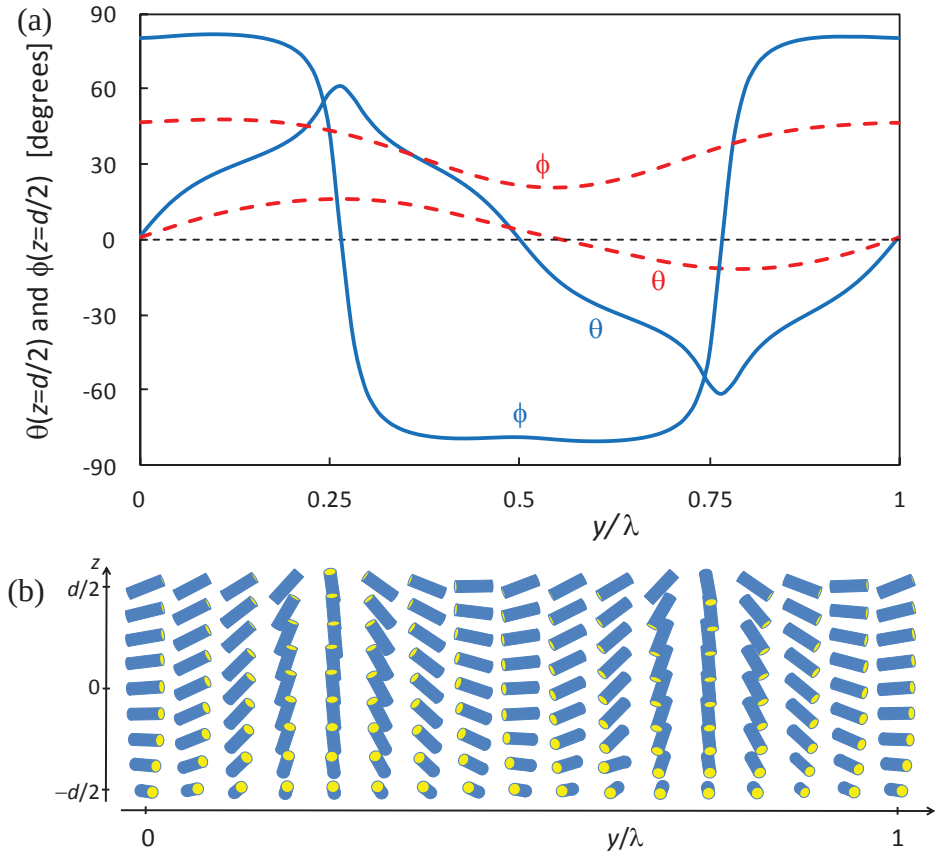

Fig. 1. (a) Periodic deformations illustrated by angles θ and ϕ adjacent to the upper electrode varying with the reduced coordinate y/λ perpendicular to the stripes. Cell A. Dashed line – Type 1, U = 0.55 V, continuous line – Type 2, U = 0.80 V, (b) Director field within a single stripe of Type 2. Cell A, U = 0.80 V

The hysteretic behaviour is shown in Fig. 2 where the amplitude of the angle $\theta(z = d/2)$ is plotted as a function of voltage. Figs. 3 and 4 exemplify the voltage dependence of the spatial period and of the angle ψ, respectively.

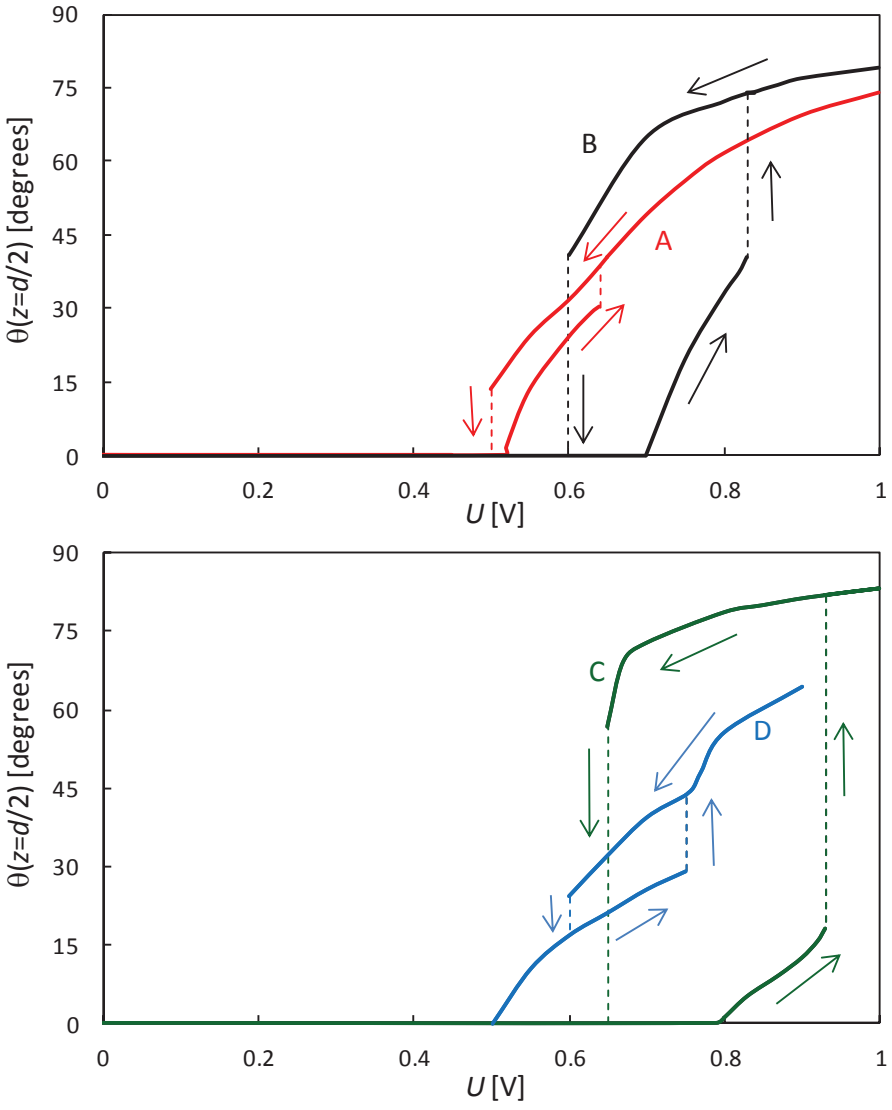

Fig. 2. Amplitude of the angle θ adjacent to the upper electrode as a function of voltage plotted for all four layers

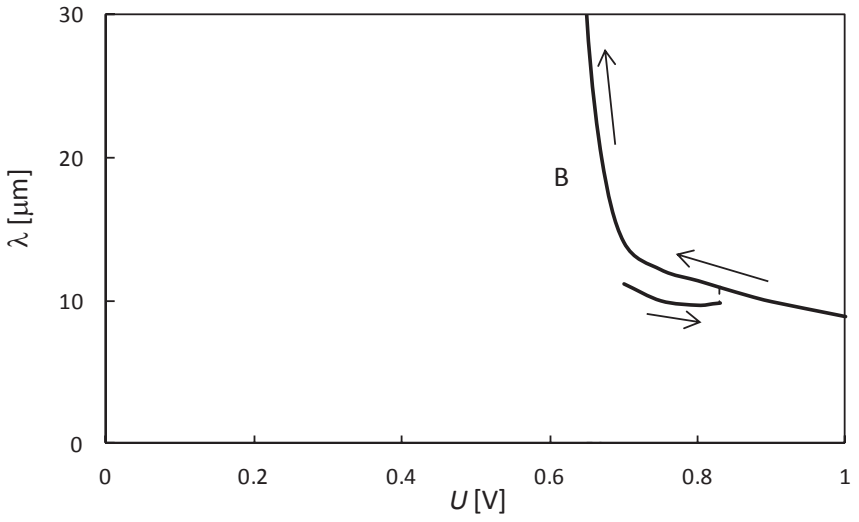

Fig. 3. Spatial period of the two-dimensional deformations in the layer B as a function of voltage. The lower branch corresponds to the Type 1 of patterns, the upper branch concerns the Type 2

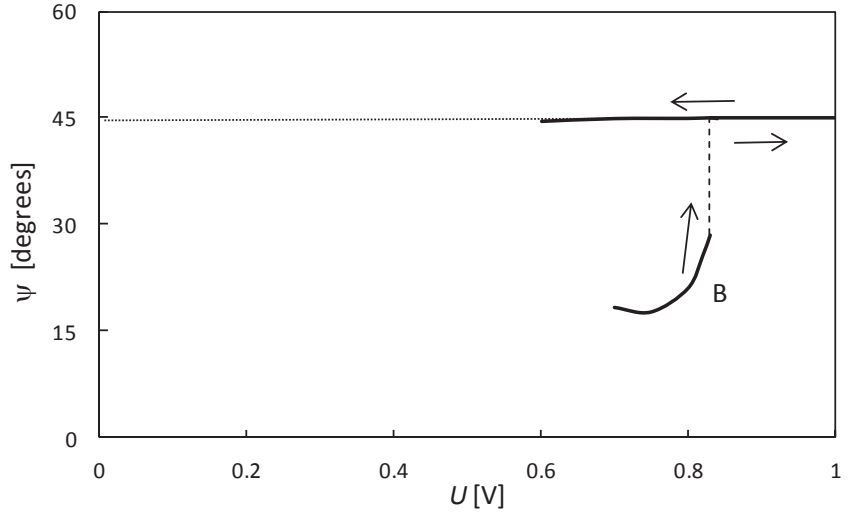

Fig. 4. Orientation of the stripes determined by the angle ψ as a function of voltage. Cell B. The lower branch corresponds to the Type 1 of patterns, the upper branch concerns the Type 2

The stripes of Type 2 widened when the bias voltage was decreased. Two halves of the stripe could be distinguished. Deformation in the halves were uniform and had opposite directions, i.e. the halves differed in signs of polar and azimuthal angles. The halves were separated by thin regions where the polar angle θ took significant values and the azimuthal angle ϕ changed its sign. At sufficiently low voltage the spatial period λ tended to infinity, which means that the uniform deformation in one half, coherent with the tilt angle θ_s, spread over the whole layer.

4. SUMMARY

The four layers considered in this paper differed in thickness and in boundary conditions, in particular in the anisotropy of the anchoring strengths. Differences in anchoring strengths are particularly significant when the nematic possesses flexoelectric properties. They are responsible for different threshold voltages and different spatial periods. Nevertheless qualitative similarities between patterns observed in the four layers are evident. In each case the two types of stripes were found and rapid transitions with hysteresis between them were detected. The results agree qualitatively with experimental observations which showed the existence of stripes oriented at the angle $\psi < 45°$ [10]. The director distributions in the stripes of both types found here are similar to the structures arising in the non-twisted planar layers which were simulated in our earlier work [27]. Simultaneously they are different from the structures of patterns arising in magnetic field which were simulated in [25] and denoted as X and Y stripes.

REFERENCES

[1] Blinov L.M., Chigrinov V.G. 1996. Electrooptical Effects in Liquid Crystal Materials. New York: Springer.
[2] Yang D.-K., Wu S.-T. 2006. Fundamentals of liquid crystal devices. John Wiley & Sons Ltd.
[3] Meyer R.B. 1969. Piezoelectric effects in liquid crystals. Phys Rev Lett. 22: 918-921.
[4] Buka A., Eber N. editors, 2012. Flexoelectricity in Liquid Crystals. Theory, Experiments and Applications. London: Imperial College Press.
[5] Harden J., Mbanga B., Eber N., Fodor-Csorba K., Sprunt S., Gleeson J.T., Jakli A. 2006. Giant flexoelectricity of bent-core nematic liquid crystals. Phys. Rev. Lett. 97: 157802.

[6] Jákli A. 2013. Liquid crystals of the twenty-first century – nematic phase of bent-core molecules. Liq Cryst Rev. 1:65-82.
[7] Derfel G., Buczkowska M. 2015. Electric field induced deformations of twisted flexoelectric nematic layers. Liq. Cryst. 42: 1213-1220.
[8] Vistin L.K. 1970. Electrostructural effect and optical properties of a certain class of liquid crystals. Sov. Phys. Crystallogr. 15: 514-515.
[9] Barnik M.I., Blinov L.M., Trufanov A.N., Umanski B.A. 1977. Flexoelectric domains in nematic liquid crystals. Sov. Phys. JETP 45: 195-198.
[10] Umanskil B.A., Chigrinov V.G., Blinov L.M., Podyachev Yu.B. 1981. Flexoelectric effect in twisted liquid-crystal structures. Sov. Phys. JETP 54: 694-699.
[11] Petrov A.G., Ionescu A.Th., Versace C., Scaramuzza N. 1995. Investigation of flexoelectric properties of a palladium-containing nematic liquid crystal, Azpac, and its mixtures with MBBA. Liq. Cryst. 19: 169-178.
[12] Marinova Y., Hinov H.P., Petrova A.G. 2005. Longitudinal flexoelectric domains in BMAOB nematic layers under the joint action of dc and ac voltages. J. Optoelectronics and Adv. Mater. 7: 277-280.
[13] Lonberg F., Meyer R.B. 1985. New ground state for the Splay-Fréedericksz transition in a polymer nematic liquid crystal. Phys. Rev. Lett. 55: 718-721.
[14] Srajer G., Fraden S., Meyer R.B. 1989. Field-induced nonequilibrium periodic structures in nematic liquid crystals: Nonlinear study of the twist Frederiks transition. Phys. Rev. A 39: 4828-4834.
[15] Frisken B.J., Palffy-Muhoray P. 1989. Effect of a transverse electric field in nematics: induced biaxiality and the bend Freedericksz transition. Liq. Cryst. 5: 623-631.
[16] Lavrentovich O.D. Pergamenshchik V.M. 1990. Periodic domain structures in thin hybrid nematic layers. Mol. Cryst. Liq. Cryst. 179: 125-132.
[17] Scheffer T., Nehring J. 1997. Supertwisted nematic (STN) liquid crystal displays. Annu. Rev. Mater. Sci. 27: 555-583.
[18] Hinov H.P., Bivas I., Mitov M.D., Shoumarov K., Marinov Y. 2003. A further experimental study of parallel surface-induced flexoelectric domains (PSIFED) (flexo-dielectric walls). Liq. Cryst. 30: 1293-1317.
[19] Bobylev Y.P., Chigrinov V.G., Pikin S.A. 1979. Threshold flexoelectric effect in nematic liquid crystal. J. Phys. Colloques. 40: C3-331-C3-333.
[20] Schiller P., Pelzl G., Demus D. 1990. Analytical theory for flexo-electric domains in nematic layer. Cryst. Res. Technol. 25: 111-116.
[21] Barbero G., Miraldi E., Oldano C. 1988. Critical values of the elastic-constant ratio for the periodic twist-splay distortion in nematic liquid crystals. Phys. Rev. A 38: 519-521.
[22] Derfel G. 1992. Stability of the periodic deformations in planar nematic layers. Liq. Cryst. 11: 431-438.
[23] Krzyżański D., Derfel G. 2000. Magnetic-field-induced periodic deformations in planar nematic layers. Phys Rev E 61: 6663-6668.

[24] Krzyżański D., Derfel G. 2001. Structure of spontaneous periodic deformations in hybrid aligned nematic layers. Phys. Rev. E 63: 021702-1 - 021702-9.
[25] Krzyżański D., Derfel G. 2002. Periodic deformations induced by a magnetic field in planar twisted nematic layers. Liq. Cryst. 29: 951-959.
[26] Derfel G., Krzyżański D. 2004. Influence of the surface tilt angle on the spatially periodic distortions in super-twisted nematic displays. J. appl. phys. 95: 3535-3540.
[27] Derfel G., Buczkowska M. 2011. Numerical study of flexoelectric longitudinal domains. Mol. Cryst. Liq. Cryst. 547: 213-221.

DWUWYMIAROWE ODKSZTAŁCENIA SKRĘCONYCH WARSTW NEMATYKÓW FLEKSOELEKTRYCZNYCH

Streszczenie

Przeprowadzono symulacje wywołanych polem elektrycznym odkształceń występujących w skręconych warstwach nematyków posiadających właściwości fleksoelektryczne. Ich celem było porównanie deformacji dwuwymiarowych z deformacjami jednowymiarowymi tych samych warstw, opisanymi we wcześniejszym artykule. Stwierdzono, że struktury przestrzennie okresowe mają niższą energię niż deformacje jednowymiarowe.